

## Durham Research Online

---

### Deposited in DRO:

24 April 2017

### Version of attached file:

Accepted Version

### Peer-review status of attached file:

Peer-reviewed

### Citation for published item:

Katus, T. and Grubert, A. and Eimer, M. (2015) 'Electrophysiological evidence for a sensory recruitment model of somatosensory working memory.', *Cerebral cortex.*, 25 (12). pp. 4697-4703.

### Further information on publisher's website:

<https://doi.org/10.1093/cercor/bhu153>

### Publisher's copyright statement:

This is a pre-copyedited, author-produced version of an article accepted for publication in *Cerebral cortex* following peer review. The version of record Katus, T. and Grubert, A. and Eimer, M. (2015) 'Electrophysiological evidence for a sensory recruitment model of somatosensory working memory.', *Cerebral cortex.*, 25(12): 4697-4703 is available online at: <https://doi.org/10.1093/cercor/bhu153>.

### Additional information:

---

### Use policy

The full-text may be used and/or reproduced, and given to third parties in any format or medium, without prior permission or charge, for personal research or study, educational, or not-for-profit purposes provided that:

- a full bibliographic reference is made to the original source
- a [link](#) is made to the metadata record in DRO
- the full-text is not changed in any way

The full-text must not be sold in any format or medium without the formal permission of the copyright holders.

Please consult the [full DRO policy](#) for further details.



**Electrophysiological evidence for a sensory recruitment  
model of somatosensory working memory**

Journal:	<i>Cerebral Cortex</i>
Manuscript ID:	CerCor-2014-00343.R2
Manuscript Type:	Original Articles
Date Submitted by the Author:	n/a
Complete List of Authors:	Katus, Tobias; Birkbeck College, Psychology Grubert, Anna; Birkbeck College, Psychology Eimer, Martin; Birkbeck College, Psychology
Keywords:	Electroencephalography (EEG), Selective Attention, Somatosensation, Working memory (WM), Event-related potentials (ERPs)

1  
2  
3  
4  
5  
6  
7  
8  
9  
10  
11  
12  
13  
14  
15  
16  
17  
18  
19  
20  
21  
22  
23  
24  
25  
26  
27  
28  
29  
30  
31  
32  
33  
34  
35  
36  
37  
38  
39  
40  
41  
42  
43  
44  
45  
46  
47  
48  
49  
50  
51  
52  
53  
54  
55  
56  
57  
58  
59  
60

1     *Full Manuscript Title*

2     **Electrophysiological evidence for a sensory recruitment model of**

3     **somatosensory working memory**

5     *Running Title*

6     **Sensory recruitment in tactile working memory**

8     *Authors and Affiliations:* Tobias Katus<sup>a</sup>, Anna Grubert<sup>a</sup> & Martin Eimer<sup>a</sup>

9     <sup>a</sup>Department of Psychology, Birkbeck College, University of London, London

10    WC1E 7HX, United Kingdom.

12    *Corresponding Author:* Tobias Katus

13    Dept. of Psychological Sciences, Birkbeck College, University of London

14    Malet Street, London WC1E 7HX

15    Phone: +44(0)20 7631 6522, Email: [t.katus@bbk.ac.uk](mailto:t.katus@bbk.ac.uk)

19    *Conflict of Interest:* The authors declare no competing financial interests.

22

**Abstract**

Sensory recruitment models of working memory assume that information storage is mediated by the same cortical areas that are responsible for the perceptual processing of sensory signals. To test this assumption, we measured somatosensory event-related brain potentials (ERPs) during a tactile delayed match-to-sample task. Participants memorized a tactile sample set at one task-relevant hand to compare it with a subsequent test set on the same hand. During the retention period, a sustained negativity (tactile contralateral delay activity, tCDA) was elicited over primary somatosensory cortex contralateral to the relevant hand. The amplitude of this component increased with memory load and was sensitive to individual limitations in memory capacity, suggesting that the tCDA reflects the maintenance of tactile information in somatosensory working memory. The tCDA was preceded by a transient negativity (N2cc component) with a similar contralateral scalp distribution, which is likely to reflect selection of task-relevant tactile stimuli at the encoding stage. The temporal sequence of N2cc and tCDA components mirrors previous observations from ERP studies of working memory in vision. The finding that the sustained somatosensory delay period activity varies as a function of memory load supports a sensory recruitment model for spatial working memory in touch.

41

42

**Introduction**

Working memory (WM) is responsible for the active maintenance of information that is no longer perceptually present. Visual and tactile working memory are both assumed to be based on distributed neural networks that include prefrontal

1  
2  
3  
4  
5  
6  
7  
8  
9  
10  
11  
12  
13  
14  
15  
16  
17  
18  
19  
20  
21  
22  
23  
24  
25  
26  
27  
28  
29  
30  
31  
32  
33  
34  
35  
36  
37  
38  
39  
40  
41  
42  
43  
44  
45  
46  
47  
48  
49  
50  
51  
52  
53  
54  
55  
56  
57  
58  
59  
60

cortex (PFC) and modality-specific perceptual areas. The activation of PFC during the maintenance of visual and tactile stimuli in working memory is well established (Curtis and D'Esposito 2003; Curtis, Rao, D'Esposito 2004; Fuster and Alexander 1971; Kostopoulos, Albanese, Petrides 2007; Romo and Salinas 2003; Postle 2005). Additionally, modality-specific visual (Harrison and Tong 2009; Supèr, Spekreijse, Lamme 2001) or somatosensory areas (e.g., Kaas et al. 2013; Zhou and Fuster 1996) show persistent activation during the retention of visual or tactile stimuli. Although the exact role of this delay-period activity in visual areas during working memory maintenance and their link to selective visual attention are still debated (e.g., van Dijk et al. 2010; Lewis-Peacock et al. 2012; Postle et al. 2013), its existence has led to the “sensory recruitment” model of working memory (D'Esposito 2007; Harrison and Tong 2009; Pasternak and Greenlee 2005; Postle 2006). This model postulates that perceptual brain regions which are responsible for the sensory processing of visual or tactile stimuli are also involved in working memory storage. The sustained activation of perceptual areas might be particularly important when working memory tasks require the maintenance of detailed sensory information (e.g., Lee, Kravitz, Baker 2013; see also Sreenivasan, Curtis, D'Esposito 2014).

Support for the sensory recruitment model comes from ERP studies of visual working memory (e.g., Vogel, McCollough, Machizawa 2005; Vogel and Machizawa 2004). In these studies, bilateral sample displays were followed after a retention interval by test displays, and participants had to match sample and test objects on one side of these displays. A sustained negativity at posterior electrodes contralateral to the side of the memorized objects (contralateral delay activity, CDA) started 300 ms after sample onset and persisted throughout the retention interval. The fact that this CDA component is sensitive to manipulations of visual working memory load and to individual differences in working memory capacity strongly suggests that the CDA

directly reflects the maintenance of visual information in working memory. The contralateral nature and posterior scalp topography of the CDA is consistent with neural generators in extrastriate visual areas (McCollough, Machizawa, Vogel 2007), in line with the sensory recruitment model. The CDA is typically preceded by an N2pc component that emerges around 200 ms post-stimulus, has a similar posterior scalp topography (e.g. McCollough, Machizawa, Vogel 2007), and reflects the attentional selection and encoding of task-relevant objects in ventral visual cortex (Eimer 1996; Luck and Hillyard 1994).

While ERP markers of visual working memory are well established, corresponding electrophysiological correlates of tactile working memory have not yet been described. Here, we demonstrate the existence of two somatosensory ERP components that are elicited during the encoding and maintenance of tactile stimuli in working memory, and both show modality-specific topographies over primary somatosensory cortex. We employed a task that was modelled on the delayed match-to-sample task used in earlier studies of visual working memory (e.g., Vogel, McCollough, Machizawa 2005; Vogel and Machizawa 2004). On each trial, a set of tactile sample stimuli was followed after a 2000 ms retention period by tactile test stimuli. Sample and test stimuli were delivered simultaneously to both hands, but the memory task had to be performed for one of these hands only. Participants had to encode and maintain tactile sample stimuli on the currently task-relevant hand, and to match them to subsequent test stimuli on the same relevant hand. On low-load trials, a single tactile stimulus had to be maintained and matched. On high-load trials, two tactile pulses had to be memorized.

Results revealed the existence of two somatosensory ERP components that have not yet been described in the literature on tactile attention and working memory. During the retention interval, a sustained tactile contralateral delay activity (tCDA)

1  
2  
3  
4  
5  
6  
7  
8  
9  
10  
11  
12  
13  
14  
15  
16  
17  
18  
19  
20  
21  
22  
23  
24  
25  
26  
27  
28  
29  
30  
31  
32  
33  
34  
35  
36  
37  
38  
39  
40  
41  
42  
43  
44  
45  
46  
47  
48  
49  
50  
51  
52  
53  
54  
55  
56  
57  
58  
59  
60

emerged with a modality-specific scalp distribution over somatosensory areas. This tCDA component was sensitive to memory load and to individual differences in tactile working memory capacity. It was preceded by a central contralateral negativity (N2cc component) with a similar modality-specific topography that was also modulated by working memory load. Analogous to the visual N2pc and CDA, these N2cc and tCDA components reflect the spatially selective encoding and maintenance of task-relevant information in tactile working memory.

**Materials and Methods**

**Participants**

Eighteen neurologically unimpaired paid adult participants were tested. The study was conducted in accordance with the Declaration of Helsinki, and was approved by the Psychology Ethics Committee, Birkbeck College. All participants gave informed written consent prior to testing. Two participants were excluded from analysis because their tactile WM capacity measured by Cowan's K (Cowan 2001) was below 1. Sixteen participants remained in the sample (mean age 32 years, range 25-44 years, 3 male, 13 right-handed).

**Stimuli and task design**

Participants were seated in a dimly lit recording chamber, viewing a monitor showing a central white fixation cross against a black background. Both hands were covered from sight and were placed on a table at a distance of approximately 40 cm. Eight mechanical tactile stimulators were attached to the distal phalanges of the index, middle, ring and small fingers of the left and right hand. Stimulators were driven by an eight-channel sound card (M-Audio, Delta 1010LT) and custom-built amplifiers, controlled by Matlab (MathWorks, Natick, MA). Continuous white noise

125 was delivered via headphones to mask sounds produced by the tactile stimulators.

126 All tactile stimuli were 100 Hz sinusoids (duration: 200 ms; intensity: 0.37 N).

127 Figure 1 illustrates the experimental procedure. Each trial started with a set of  
128 tactile sample stimuli that were delivered simultaneously to the left and right hand.  
129 After a 2000 ms retention period, a set of tactile test stimuli was presented  
130 simultaneously to both hands. Prior to the start of each block, instructions displayed  
131 on the monitor informed participants whether the left or right hand was relevant in the  
132 upcoming block. Participants had to decide whether sample and test stimulus  
133 locations on this hand were identical (match trials) or different (mismatch trials). The  
134 task-relevant hand was swapped after each experimental block. Two load conditions  
135 were randomized within each block. In the *low-load condition*, one sample pulse was  
136 presented with equal probability to one of the four fingers of the left hand and the  
137 right hand. On match trials, the test pulse was delivered to the same finger of the  
138 relevant hand as the sample pulse. On mismatch trials, one of the three other fingers  
139 on that hand was stimulated at test. In the *high-load condition*, two sample pulses  
140 were presented to two randomly selected fingers of the left hand and the right hand,  
141 respectively. On match trials, test pulses were delivered to the same two fingers of  
142 the relevant hand. On mismatch trials, at least one of the two test pulses was  
143 presented to a different finger of that hand. Because one of the two sample locations  
144 could be repeated at test on mismatch trials, participants had to retain the location of  
145 both sample stimuli on the relevant hand to perform the task in the high-load  
146 condition. Match and mismatch trials were equiprobable. On the currently task-  
147 irrelevant hand, sample and test stimuli were also presented at matching or  
148 mismatching locations, and this was independent of whether there was a match or  
149 mismatch on the relevant hand.



Participants signalled a match or mismatch between sample and test on the relevant hand with a vocal response (“a” for match and “e” for mismatch) that was recorded with a headset microphone between 200 ms and 1700 ms after test stimulus offset. A question mark replaced the fixation cross on the monitor during this period. The interval between the offset of this question mark and the onset of the sample pulses on the next trial varied between 800 and 1100 ms. The experiment included ten blocks of 48 trials, with twelve trials per block for each of the four combinations of high versus low load trials and match versus mismatch trials. Instructions emphasized accuracy over speed, and the need to avoid head and arm movements and to maintain central gaze fixation. Feedback on hit and correct rejection rates was provided after each block. Two training blocks were run prior to the first experimental block.

Insert Figure 1 about here

**Processing of EEG data**

EEG data, sampled at 500 Hz using a BrainVision amplifier, were DC-recorded from 64 Ag/AgCl active electrodes at standard locations of the extended 10-20 system. Two electrodes at the outer canthi of the eyes monitored lateral eye movements (horizontal electrooculogram, HEOG) and electrodes sites TP9/10 were used as mastoid references. Continuous EEG data was referenced to the left mastoid during recording, and was offline re-referenced to the arithmetic mean of both mastoids and submitted to a 40Hz low-pass finite impulse response filter (Blackman

175 window, filter order 666). EEG epochs for the 2000 ms interval following sample  
176 stimulus onset were computed relative to a 200 ms pre-stimulus baseline. Blind  
177 source separation of EEG data was performed with the Independent Component  
178 Analysis (ICA) algorithm implemented in the EEGLab toolbox (Delorme and Makeig  
179 2004; Delorme, Sejnowski, Makeig 2007). Independent components related to  
180 artifacts at anterior scalp regions (in particular, eye movements and blinks), were  
181 identified by visual inspection and subtracted from the EEG data. To obtain reliable  
182 ICA decompositions, a copy of the data was segmented into eight 250 ms frames  
183 covering the 2000 ms retention period. These frames were corrected using whole-  
184 epoch baselines to achieve data stationarity (cf., Groppe, Makeig, Kutas 2009)  
185 without high-pass filtering, which would have removed slow brain potentials. The  
186 copy was discarded after ICA decompositions had been applied to the original data  
187 set. Epochs with lateral eye movements that escaped ICA artifact correction were  
188 identified and removed with a differential step function on the bipolarized HEOG (step  
189 width 100 ms, threshold 24  $\mu$ V). The resulting HEOG waveforms contained no  
190 systematic eye gaze deflections towards the task-relevant hand (Figure 2, bottom  
191 panel). After artifact rejection and elimination of trials with incorrect responses, 90.2%  
192 of all epochs were retained for statistical analyses (low load: 93.4%; high load:  
193 87.1%).

## 195 Results

### 196 Behavioral performance

197 Participants responded correctly on 97.1% of all low-load trials and 90.4% of  
198 all high-load trials. Sensitivity indices ( $d'$ ) were analysed in a two-way repeated  
199 measures ANOVA with the factors memory load (low, high) and relevant hand (left,  
200 right). Performance was reduced with high load relative to low load ( $F(1,15) = 71.728$ ,

$p < 10^{-6}$ ), and did not differ between blocks where the left or right hand was relevant ( $F(1,15) = 1.081, p > 0.3$ ). A significant memory load x relevant hand interaction ( $F(1,15) = 6.222, p = 0.025$ ) was due to the fact that the performance decrement with high as compared to low memory load was larger when the memory task was performed with the left hand (8.5%) relative to blocks where the right hand was relevant (4.9%).

Mean vocal reaction times (RTs) in trials with correct responses were faster in the low-load relative to the high-load condition (799 ms versus 817 ms; main effect of memory load:  $F(1,15) = 8.801, p = 0.010$ ). RTs did not differ between blocks where the left or right hand was task-relevant ( $F(1, 15) = 1.846, p > 0.1$ ). The memory load x relevant hand interaction was significant ( $F(1,15) = 5.25, p = 0.037$ ), as the RT costs for the low-load versus high-load condition were larger when the memory task was performed with the right hand (26 ms) relative to blocks where the left hand was relevant (10 ms). In other words, there was an asymmetric speed-accuracy tradeoff between the two hands for task performance in the high-load versus low-load condition.

**Electrophysiological data**

Figure 2 shows ERP waveforms averaged across lateral central electrodes (FC3/4, FC5/6, C3/4, C5/6, CP3/4, CP5/6) contralateral and ipsilateral to the task-relevant hand for the 2000 ms interval between the bilateral sample stimulus and the subsequent test stimulus. Results are shown separately for the low-load and high-load conditions. Following the early sensory-evoked ERP components to the sample stimulus, ERP waveforms were characterized by a gradually developing sustained negativity that reached its maximal amplitude immediately before the onset of the test

stimuli. This sustained negativity that was present at contralateral as well as ipsilateral electrodes reflects the Contingent Negative Variation (CNV; see Birbaumer et al. 1990) that is elicited in anticipation of expected task-relevant events such as the test stimulus set used in this study. More importantly, sample stimuli triggered a transient enhanced negativity contralateral to the task-relevant hand. This N2cc component emerged around 180 ms after sample stimulus onset, and its amplitude was larger in the high-load as compared to the low-load condition. The N2cc was followed by a sustained contralateral negativity (tCDA) that remained present throughout the retention period. This tCDA component was larger when two tactile stimuli had to be memorized relative to the low load condition. The topographical maps in Figure 2 illustrate the scalp distribution of N2cc and tCDA components in the low-load and high-load conditions. Data shown in these maps were collapsed across blocks where the left or right hand was task-relevant by flipping ERPs at contralateral electrodes in blocks with a left-hand memory task over the midline. Both N2cc and tCDA components were maximal over somatosensory areas in the postcentral gyrus and adjacent parietal regions (see also Figure 4 below).

Insert Figure 2 about here

Difference waveforms were computed by subtracting ERPs ipsilateral to the currently task-relevant hand from contralateral ERPs. Statistical tests were conducted on mean amplitudes of these difference waves for a time window centered on the N2cc component (180-260 ms post-stimulus), and a second window centered on the

1  
2  
3  
4  
5  
6  
7  
8  
9  
10  
11  
12  
13  
14  
15  
16  
17  
18  
19  
20  
21  
22  
23  
24  
25  
26  
27  
28  
29  
30  
31  
32  
33  
34  
35  
36  
37  
38  
39  
40  
41  
42  
43  
44  
45  
46  
47  
48  
49  
50  
51  
52  
53  
54  
55  
56  
57  
58  
59  
60

tCDA (300-2000 ms). Difference values that statistically differ from zero mark the presence of reliable lateralized components in the ERP waveforms. The N2cc was present in both the low-load ( $t(15) = -5.593, p < 10^{-4}$ ) and high-load condition ( $t(15) = -7.037, p < 10^{-5}$ ). N2cc amplitudes were significantly larger with high relative to low memory load ( $t(15) = 4.235, p < 10^{-3}$ ). The tCDA component was present with low load ( $t(15) = -2.951, p = 0.010$ ) as well as with high memory load ( $t(15) = -6.126, p < 10^{-4}$ ). Similar to the N2cc, tCDA amplitudes were significantly larger in the high-load relative to the low-load condition ( $t(15) = 3.801, p = 0.002$ ).

An additional analysis of mean amplitudes in the tCDA time window obtained for the unsubtracted ERP waveforms revealed a main effect of contralaterality (electrodes contralateral versus ipsilateral to the task-relevant hand;  $F(1,15) = 38.006, p < 10^{-4}$ ) that interacted with load ( $F(1,15) = 14.448, p = 0.002$ ), due to the fact that the tCDA was larger in the high-load condition. There was also a main effect of load ( $F(1,15) = 14.862, p=0.002$ ), with larger CNV components with high memory load. This load-dependent modulation of CNV amplitudes was reliable at contralateral as well as ipsilateral electrodes  $t(15) = -4.500$  and  $-2.481, p < 0.001$  and  $0.026$ , respectively).

Tactile working memory capacity was calculated for each individual participant on the basis of their performance in the high-load condition, using the formula  $K = (hits + correct\ rejections - 1) \times 2$ , where 2 denotes memory set size in this condition (Cowan 2001). As illustrated in Figure 3, individual memory capacity was reliably correlated with the difference of tCDA amplitudes between the high-load and low-load conditions ( $r = -0.640, p = 0.008$ ). Participants with higher tactile working memory capacity showed a more pronounced increase of the tCDA component on trials with high versus low memory load than participants with lower capacity. No correlation

was found between individual K values and the difference of N2cc amplitudes between high- and low-load conditions ( $p > 0.7$ ).

To obtain additional evidence for a link between tCDA amplitudes and behavioral performance at the level of individual trials in the high-load condition, we computed tCDA components in the high-load condition separately for trials with vocal RTs above and below the median RT (with RT median splits conducted individually for each participant and trial condition). Trials with fast responses were more accurate than slow response trials (Cowan's K: fast = 1.786, slow = 1.453;  $t(15) = 6.362$ ,  $p < 10^{-4}$ ). Critically, tCDA amplitudes were larger for fast as compared to slow response trials ( $-0.749 \mu V$  versus  $-0.594 \mu V$ ), and this amplitude difference was significant ( $t(15) = -2.564$ ,  $p = 0.022$ ).

287

288 -----

289 Insert Figure 3 about here

290 -----

291

An additional current source density (CSD) analysis was conducted to further illustrate the modality-specific scalp topographies of the N2cc and tCDA components, and to demonstrate that the selection of lateral central electrodes for the analysis of these components was appropriate. ERP data were collapsed across the low- and high-load conditions, after conversion of scalp potentials to surface Laplacians ( $\lambda = 10^{-5}$ , iterations = 50,  $m = 4$ ; cf. Tenke and Kayser 2012). This transformation minimizes effects of volume conduction from remote sources, and leads to a reference-independent representation of EEG/ERP data. CSD topographies provide a conservative estimate of the neural generator patterns that

contribute to scalp-recorded ERPs (Nunez and Westdorp 1994; Tenke and Kayser 2012). Robust lateralized effects were found over somatosensory brain regions (Figure 4), as demonstrated by significant differences of contra- minus ipsilateral activity recorded at central electrodes in the time window of N2cc ( $t(15) = -6.476$ ,  $p < 10^{-4}$ ) and tCDA ( $t(15) = -4.066$ ,  $p = 0.001$ ). Apart from an almost significant contralateral positivity at anterior regions during the N2cc time window ( $t(15) = 2.107$ ,  $p = 0.052$ ), no statistically reliable lateralization was evident over posterior (electrodes P3/4, P5/6, PO3/4, PO7/8) and anterior (electrodes AF3/4, AF7/8, F3/4, F5/6) scalp regions (all  $ps > 0.2$ ; see Figure 4).

Insert Figure 4 about here

Discussion

We employed a tactile memory task that was modelled on the delayed match-to-sample task used in previous research on visual working memory (e.g., Vogel and Machizawa 2004) to identify ERP correlates of the selection and maintenance of task-relevant tactile stimuli. When participants memorized the spatial locations of one or two tactile sample pulses on the left or the right hand, an enhanced negativity with a centroparietal focus emerged contralateral to the hand where the memorized tactile sample was delivered. This tCDA component was sensitive to tactile working memory load, as it was larger on trials where participants had to remember two tactile stimulus locations than when only a single tactile location had to be memorized

(Figure 2). The load-dependent increase of tCDA amplitudes was more pronounced for participants with higher tactile working memory capacity than for individuals whose capacity (measured by Cowan's K) was closer to 1 (Figure 3), mirroring previous findings for the visual CDA component (Vogel and Machizawa 2004). Furthermore, the tCDA component was reliably larger on trials with fast vocal responses in the high-load condition, which were also more accurate than slow responses. This demonstrates that the tCDA component is linked to behavioral performance on individual trials. These observations strongly suggest that the tCDA is an electrophysiological correlate of the maintenance of somatosensory information in tactile working memory.

Analogous to the visual CDA, which has a modality-specific topography over posterior visual cortex (McCollough, Machizawa, Vogel 2007), the tactile CDA component emerged at contralateral central electrodes. The scalp topography of the tCDA in a CSD-transformed map (Figure 4) also suggests neural generators that are located within the somatosensory system. We conclude that the tCDA component reflects the spatially selective activation of modality-specific brain regions contralateral to the task-relevant hand during the retention of tactile stimuli in working memory. These results provide new support for the sensory recruitment model, which assumes that brain regions involved in the perceptual processing of sensory stimuli are also active during the maintenance of these stimuli in working memory. It should be noted that topographical distributions of CSD-transformed scalp maps only allow relatively coarse approximations of the neural origins of components such as the tCDA, and that the exact anatomical basis of this component needs to be determined in future work.

Previous research has used transcranial magnetic stimulation (TMS; Harris et al. 2002) and EEG source reconstruction techniques in studies with human



1  
2  
3  
4  
5  
6  
7  
8  
9  
10  
11  
12  
13  
14  
15  
16  
17  
18  
19  
20  
21  
22  
23  
24  
25  
26  
27  
28  
29  
30  
31  
32  
33  
34  
35  
36  
37  
38  
39  
40  
41  
42  
43  
44  
45  
46  
47  
48  
49  
50  
51  
52  
53  
54  
55  
56  
57  
58  
59  
60

352 participants (Spitzer and Blankenburg 2011), as well as single-cell recordings in  
353 monkeys (Romo and Salinas 2003) to show that the activity of neurons in primary  
354 (SI) and secondary (SII) somatosensory cortex is modulated in tactile working  
355 memory tasks. For example, a suppression of alpha activity indicative of attentional  
356 processing was found over contralateral SI during the retention period of a  
357 vibrotactile frequency discrimination task (Spitzer and Blankenburg 2011).  
358 Asymmetric alpha band oscillations have also been suggested as the physiological  
359 basis of the visual CDA component (van Dijk et al. 2010). Indirect evidence for a  
360 recruitment of somatosensory brain areas comes from a tactile EEG study that used  
361 task-irrelevant probe stimuli presented during the retention period to examine how  
362 working memory influences somatosensory encoding (Katus, Andersen, Müller  
363 2012). The retention of locations in working memory was mirrored by spatially  
364 selective modulation of early ERP components to tactile probe stimuli with putative  
365 origins in somatosensory areas such as SII (Frot and Mauguière 1999). These lines  
366 of evidence point towards close links between the maintenance of tactile information  
367 in working memory and the spatially specific activation of early somatosensory areas.  
368 The critical new finding of the present study is the discovery of the tCDA component  
369 that reflects the maintenance of tactile information in a sustained and load-dependent  
370 manner. Because the tCDA is computed by comparing ERPs at electrodes  
371 contralateral and ipsilateral to the location of memorized tactile events, it only reflects  
372 the difference in the absolute activation of contralateral versus ipsilateral  
373 somatosensory areas, and should therefore not be interpreted as evidence that  
374 tactile working memory storage is exclusively contralateral. In fact, there is  
375 electrophysiological evidence that ipsilateral somatosensory cortex may also be  
376 involved in the maintenance of tactile pattern information (Li Hegner et al. 2007).

The tCDA component was preceded by an earlier contralateral negativity, (N2cc component) which emerged around 180 ms after sample stimulus onset. Similar to the tCDA, the N2cc showed a centroparietal scalp topography (see Figures 2 and 4), and was larger in the high-load as compared to the low-load condition. This new N2cc component is likely to represent the somatosensory equivalent of the well-known visual N2pc component. The N2pc is triggered at contralateral posterior electrodes at a similar post-stimulus latency during the attentional selection of targets among distractors in visual displays (Eimer 1996; Luck and Hillyard 1994), and precedes the CDA in visual working memory studies that employ a similar delayed match-to-sample task as the one used in the present study (e.g., Anderson, Vogel, Awh 2011; McCollough, Machizawa, Vogel 2007). The load-dependent increase of the tactile N2cc component observed in the present study mirrors previous findings for the visual N2pc, which increases in size with the number of attended objects in visual displays (e.g., Drew and Vogel 2008; Mazza and Caramazza 2011).

The absence of N2cc components in previous ERP studies of tactile spatial attention is due to the fact that instead of employing bilateral stimuli, tactile events were delivered to a single location on the left or right hand. In these studies, modality-specific components of the somatosensory event-related potential, such as the P100 or N140, were found to be larger for tactile stimuli at currently attended as compared to unattended positions (e.g., Forster and Eimer 2005), demonstrating that spatial attention enhances the sensory processing of tactile events. Analogous to the visual N2pc, which is elicited when target and distractor objects appear in both visual hemifields, measurement of the N2cc component requires that relevant and irrelevant tactile events are presented simultaneously to both hands, or to other homologous locations on the left and right side of the body. Note that the modality-specific somatosensory N2cc component found here is distinct from another ERP component

1  
2  
3  
4  
5  
6  
7  
8  
9  
10  
11  
12  
13  
14  
15  
16  
17  
18  
19  
20  
21  
22  
23  
24  
25  
26  
27  
28  
29  
30  
31  
32  
33  
34  
35  
36  
37  
38  
39  
40  
41  
42  
43  
44  
45  
46  
47  
48  
49  
50  
51  
52  
53  
54  
55  
56  
57  
58  
59  
60

403 with the same label that has been observed in stimulus-response compatibility  
404 experiments, and is linked to visuospatially guided response selection (Praamstra  
405 and Oostenveld 2003). The question whether the effects of memory load on the N2cc  
406 and tCDA components reflect load-sensitive modulations of two distinct processing  
407 stages (i.e., the attentional selection and the subsequent storage of task-relevant  
408 tactile information in working memory), or of a single memory maintenance stage that  
409 temporally overlaps with the N2cc component needs to be investigated in future  
410 studies where the demands on attentional target selection and working memory load  
411 are independently manipulated. In addition to the N2cc and tCDA components, a  
412 sustained bilateral CNV component that was observed in the interval between  
413 sample and test stimuli was also modulated by memory load. This modulation may  
414 primarily reflect differences in the preparation for the match/mismatch decision in  
415 response to the test stimulus, which is more demanding in the high-load condition.  
416 However, the presence of load effects at ipsilateral electrodes could in principle as  
417 well reflect contributions of ipsilateral somatosensory cortex to working memory  
418 maintenance (Li Hegner et al. 2007; see also van Ede, Lange, Maris 2013).

419 When considered together with the results of previous ERP investigations of  
420 visual working memory (Anderson, Vogel, Awh 2011; McCollough, Machizawa, Vogel  
421 2007; Vogel, McCollough, Machizawa 2005; Vogel and Machizawa 2004), the current  
422 findings reveal striking similarities between the mechanisms that underlie the spatial  
423 selection and selective maintenance of sensory stimuli in vision and touch. During  
424 both visual and tactile working memory tasks, two contralateral ERP components are  
425 elicited successively, with a highly similar time course in both modalities. N2pc and  
426 N2cc components that emerge around 180 ms after sample display onset reflect  
427 spatial selection during encoding of task-relevant visual or tactile information. The  
428 subsequent CDA and tCDA components are linked to the sustained maintenance of

stored information during the retention period. The fact that the load-sensitive tCDA component observed in this study showed a topography over lateral central somatosensory areas (see Figure 4), while the visual CDA component is elicited over lateral posterior visual cortex (McCollough, Machizawa, Vogel 2007) strongly suggests that the maintenance of visual or tactile information in working memory involves the activation of distinct modality-specific regions, in line with the sensory recruitment model of working memory (D'Esposito 2007; Pasternak and Greenlee 2005; Postle 2006; Sreenivasan, Curtis, D'Esposito 2014). In both vision and touch, neural networks that mediate the perceptual processing of sensory signals contribute to the storage and maintenance of information in working memory.

## Acknowledgments

This work was funded by the Deutsche Forschungsgemeinschaft (DFG grant KA 3843/1-1). We thank Sue Nicholas for invaluable help in setting up the hardware used for tactile stimulation.

## References

- Anderson DE, Vogel EK, Awh E. 2011. Precision in visual working memory reaches a stable plateau when individual item limits are exceeded. *J Neurosci.* 31(3):1128–1138.
- Birbaumer N, Elbert T, Canavan AG, Rockstroh, B 1990. Slow potentials of the cerebral cortex and behavior. *Physiol Rev.* 70(1): 1-41.
- Cowan N. 2001. The magical number 4 in short-term memory: a reconsideration of mental storage capacity. *Behav Brain Sci.* 24(1):87-114x.

1  
2  
3  
4  
5  
6  
7  
8  
9  
10  
11  
12  
13  
14  
15  
16  
17  
18  
19  
20  
21  
22  
23  
24  
25  
26  
27  
28  
29  
30  
31  
32  
33  
34  
35  
36  
37  
38  
39  
40  
41  
42  
43  
44  
45  
46  
47  
48  
49  
50  
51  
52  
53  
54  
55  
56  
57  
58  
59  
60

453 Curtis CE, D'Esposito M. 2003. Persistent activity in the prefrontal cortex during  
454 working memory. *Trends Cogn Sci.* 7(9):415–423.

455 Curtis CE, Rao VY, D'Esposito M. 2004. Maintenance of spatial and motor codes  
456 during oculomotor delayed response tasks. *J Neurosci.* 24(16):3944–3952.

457 Delorme A, Makeig S. 2004. EEGLAB: an open source toolbox for analysis of single-  
458 trial EEG dynamics including independent component analysis. *J Neurosci*  
459 *Methods.* 134(1):9–21.

460 Delorme A, Sejnowski T, Makeig S. 2007. Enhanced detection of artifacts in EEG  
461 data using higher-order statistics and independent component analysis.  
462 *Neuroimage.* 34(4):1443–1449.

463 D'Esposito M. 2007. From cognitive to neural models of working memory. *Philos*  
464 *Trans R Soc Lond B Biol Sci.* 362(1481):761–772.

465 Drew T, Vogel EK. 2008. Neural measures of individual differences in selecting and  
466 tracking multiple moving objects. *J Neurosci.* 28(16):4183–4191.

467 Eimer M. 1996. The N2pc component as an indicator of attentional selectivity.  
468 *Electroencephalogr Clin Neurophysiol.* 99(3):225–234.

469 Forster B, Eimer M. 2005. Covert attention in touch: Behavioral and ERP evidence  
470 for costs and benefits. *Psychophysiology.* 42(2):171–179.

471 Frot M, Mauguière F. 1999. Timing and spatial distribution of somatosensory  
472 responses recorded in the upper bank of the sylvian fissure (SII area) in humans.  
473 *Cereb Cortex.* 9(8):854–863.

474 Fuster JM, Alexander GE. 1971. Neuron activity related to short-term memory.  
475 *Science.* 173(3997):652–654.

476 Groppe DM, Makeig S, Kutas M. 2009. Identifying reliable independent components  
477 via split-half comparisons. *Neuroimage.* 45(4):1199–1211.

- 1  
2  
3 478 Harris JA, Miniussi C, Harris IM, Diamond ME. 2002. Transient storage of a tactile  
4  
5 479 memory trace in primary somatosensory cortex. *J Neurosci*. 22(19):8720–8725.  
6  
7 480 Harrison SA, Tong F. 2009. Decoding reveals the contents of visual working memory  
8  
9 481 in early visual areas. *Nature*. 458(7238):632–635.  
10  
11 482 Kaas AL, van Mier H, Visser M, Goebel R. 2013. The neural substrate for working  
12  
13 483 memory of tactile surface texture. *Hum Brain Mapp*. 34(5):1148–1162.  
14  
15 484 Katus T, Andersen SK, Müller MM. 2012. Maintenance of tactile short-term memory  
16  
17 485 for locations is mediated by spatial attention. *Biol Psychol*. 89(1):39–46.  
18  
19 486 Kostopoulos P, Albanese M, Petrides M. 2007. Ventrolateral prefrontal cortex and  
20  
21 487 tactile memory disambiguation in the human brain. *Proc Natl Acad Sci USA*.  
22  
23 488 104(24):10223–10228.  
24  
25 489 Lee SH, Kravitz DJ, Baker CI. 2013. Goal-dependent dissociation of visual and  
26  
27 490 prefrontal cortices during working memory. *Nature Neurosci*. 16(8), 997–999.  
28  
29 491 Li Hegner Y, Lutzenberger W, Leiberg S, Braun C. 2007. The involvement of  
30  
31 492 ipsilateral temporoparietal cortex in tactile pattern working memory as reflected in  
32  
33 493 beta event-related desynchronization. *Neuroimage*. 37(4): 1362–1370.  
34  
35 494 Lewis-Peacock JA, Drysdale AT, Oberauer K, Postle BR. 2012. Neural evidence for a  
36  
37 495 distinction between short-term memory and the focus of attention. *J Cogn*  
38  
39 496 *Neurosci*. 24(1): 61–79.  
40  
41 497 Luck SJ, Hillyard SA. 1994. Spatial filtering during visual search: Evidence from  
42  
43 498 human electrophysiology. *J Exp Psychol Hum Percept Perform*. 20(5):1000–1014.  
44  
45 499 Mazza V, Caramazza A. 2011. Temporal brain dynamics of multiple object  
46  
47 500 processing: the flexibility of individuation. *PLoS ONE*. 6(2):e17453.  
48  
49 501 McCollough AW, Machizawa MG, Vogel EK. 2007. Electrophysiological measures of  
50  
51 502 maintaining representations in visual working memory. *Cortex*. 43(1):77–94.  
52  
53  
54  
55  
56  
57  
58  
59  
60

1  
2  
3  
4  
5  
6  
7  
8  
9  
10  
11  
12  
13  
14  
15  
16  
17  
18  
19  
20  
21  
22  
23  
24  
25  
26  
27  
28  
29  
30  
31  
32  
33  
34  
35  
36  
37  
38  
39  
40  
41  
42  
43  
44  
45  
46  
47  
48  
49  
50  
51  
52  
53  
54  
55  
56  
57  
58  
59  
60

503 Nunez PL, Westdorp AF. 1994. The surface Laplacian, high resolution EEG and  
504 controversies. *Brain Topogr.* 6(3):221–226.

505 Pasternak T, Greenlee MW. 2005. Working memory in primate sensory systems. *Nat*  
506 *Rev Neurosci.* 6(2):97–107.

507 Postle BR. 2005. Delay-period activity in the prefrontal cortex: one function is sensory  
508 gating. *J Cogn Neurosci.* 17(11):1679–1690.

509 Postle BR. 2006. Working memory as an emergent property of the mind and brain.  
510 *Neuroscience.* 139(1):23–38.

511 Postle BR, Awh E, Serences JT, Sutterer DW, D'Esposito M. 2013. The positional-  
512 specificity effect reveals a passive-trace contribution to visual short-term memory.  
513 *PLoS ONE.* 8(12): e83483.

514 Praamstra P, Oostenveld R. 2003. Attention and movement-related motor cortex  
515 activation: a high-density EEG study of spatial stimulus-response compatibility.  
516 *Brain Res Cogn Brain Res.* 16(3):309–322.

517 Romo R, Salinas E. 2003. Flutter discrimination: neural codes, perception, memory  
518 and decision making. *Nat Rev Neurosci.* 4(3):203–218.

519 Spitzer B, Blankenburg F. 2011. Stimulus-dependent EEG activity reflects internal  
520 updating of tactile working memory in humans. *Proc Natl Acad Sci USA.*  
521 108(20):8444–8449.

522 Sreenivasan KK, Curtis CE, D'Esposito M. 2014. Revisiting the role of persistent  
523 neural activity during working memory. *Trends Cogn Sci.* 18(2), 82-89.

524 Supèr H, Spekreijse H, Lamme VA. 2001. A neural correlate of working memory in  
525 the monkey primary visual cortex. *Science.* 293(5527):120–124.

526 Tenke CE, Kayser J. 2012. Generator localization by current source density (CSD):  
527 implications of volume conduction and field closure at intracranial and scalp  
528 resolutions. *Clin Neurophysiol.* 123(12):2328–2345.



- van Dijk H, van der Werf J, Mazaheri A, Medendorp WP, Jensen O. 2010. Modulations in oscillatory activity with amplitude asymmetry can produce cognitively relevant event-related responses. *Proc Natl Acad Sci USA*. 107(2): 900–905.
- van Ede F, de Lange FP, Maris E. 2013. Anticipation increases tactile stimulus processing in the ipsilateral primary somatosensory cortex. *Cereb Cortex*. Doi: 10.1093/cercor/bht111.
- Vogel EK, McCollough AW, Machizawa MG. 2005. Neural measures reveal individual differences in controlling access to working memory. *Nature*. 438(7067):500–503.
- Zhou YD, Fuster JM. 1996. Mnemonic neuronal activity in somatosensory cortex. *Proc Natl Acad Sci USA*. 93(19):10533–10537.

### Figure Legends

**Figure 1.** Illustration of the experimental setup. Participants memorized a tactile sample set at one task-relevant hand to compare it with a test set on the same hand after a 2 second retention period. Memory load was varied between trials (low load: one pulse, high load: two pulses per hand). The relevant hand (left, right) was varied between blocks. The example shown here illustrates a high-load trial where the locations of tactile sample and test stimuli (symbolized by white dots) are identical at the left hand (match), but not at the right hand (mismatch).

**Figure 2.** Grand mean ERPs elicited in the 2000 ms interval following sample stimulus onset in the low-load and high-load conditions. ERPs were averaged across



1  
2  
3  
4  
5  
6  
7  
8  
9  
10  
11  
12  
13  
14  
15  
16  
17  
18  
19  
20  
21  
22  
23  
24  
25  
26  
27  
28  
29  
30  
31  
32  
33  
34  
35  
36  
37  
38  
39  
40  
41  
42  
43  
44  
45  
46  
47  
48  
49  
50  
51  
52  
53  
54  
55  
56  
57  
58  
59  
60

lateral central electrode clusters contralateral (blue lines) and ipsilateral (red lines) to the hand where the memory task was performed. Difference maps show the topographical distribution of lateralized effects in the N2cc (bottom) and tCDA (top) time windows. These maps represent the amplitude difference of contralateral minus ipsilateral recordings, collapsed across blocks where the memory task was performed with the left or right hand. Enhanced contralateral negativities are shown in blue. The two bottom panels show difference waveforms for the low-load and high-load condition, obtained by subtracting electrodes ipsilateral to the task-relevant hand from contralateral electrodes, and HEOG difference waveforms, calculated by subtracting HEOG electrodes ipsilateral to the task-relevant hand from contralateral electrodes after artifact rejection. In these HEOG difference waves, any eye movements towards the task-relevant hand would be reflected by negative (downward) HEOG deflections.

**Figure 3.** Correlation of individual participant’s tactile working memory capacity K (x-axis) and the increase of tCDA amplitudes in the high-load relative to the low-load condition measured for each participant (y-axis). K was calculated on the basis of individual performance in the high-load condition.

**Figure 4.** Grand mean current source density (CSD) topographical maps, showing the scalp distribution of lateralized effects in the N2cc and tCDA time windows. These maps represent the amplitude difference of contralateral minus ipsilateral recordings, collapsed across blocks where the memory task was performed with the left or right hand, and averaged across the low- and high-load conditions. Six electrodes at lateral central scalp regions (black dots) were averaged for each recording cluster

1  
2  
3 579 (contra- and ipsilateral to the task-relevant hand). The presence of lateralized effects  
4  
5 580 was also tested for different sets of electrodes over anterior (white triangles) and  
6  
7 581 posterior (white crosses) scalp areas. Reliable lateralized effects were present only  
8  
9 582 for the central electrode cluster.  
10  
11  
12  
13  
14  
15  
16  
17  
18  
19  
20  
21  
22  
23  
24  
25  
26  
27  
28  
29  
30  
31  
32  
33  
34  
35  
36  
37  
38  
39  
40  
41  
42  
43  
44  
45  
46  
47  
48  
49  
50  
51  
52  
53  
54  
55  
56  
57  
58  
59  
60

For Peer Review

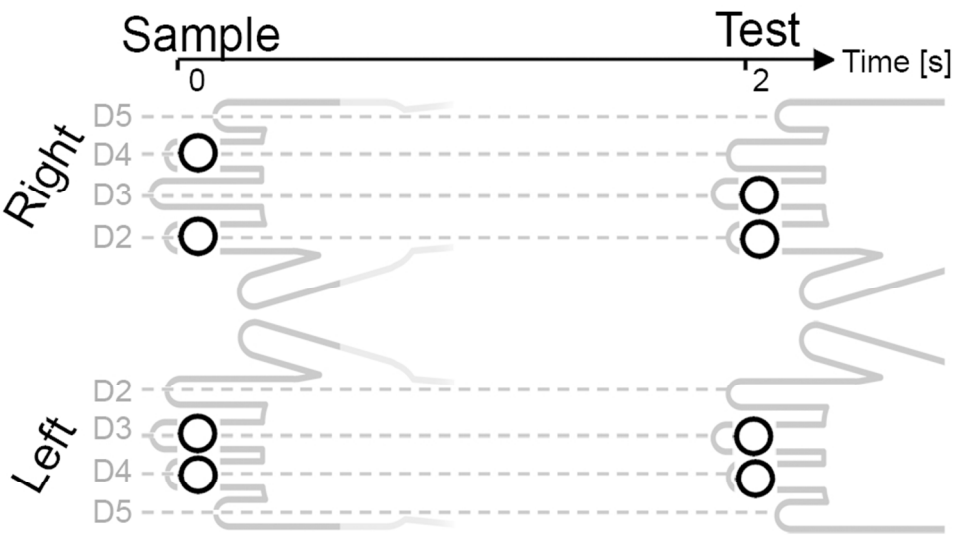


Figure 1. Illustration of the experimental setup. Participants memorized a tactile sample set at one task-relevant hand to compare it with a test set on the same hand after a 2 second retention period. Memory load was varied between trials (low load: one pulse, high load: two pulses per hand). The relevant hand (left, right) was varied between blocks. The example shown here illustrates a high-load trial where the locations of tactile sample and test stimuli (symbolized by white dots) are identical at the left hand (match), but not at the right hand (mismatch).

86x50mm (300 x 300 DPI)

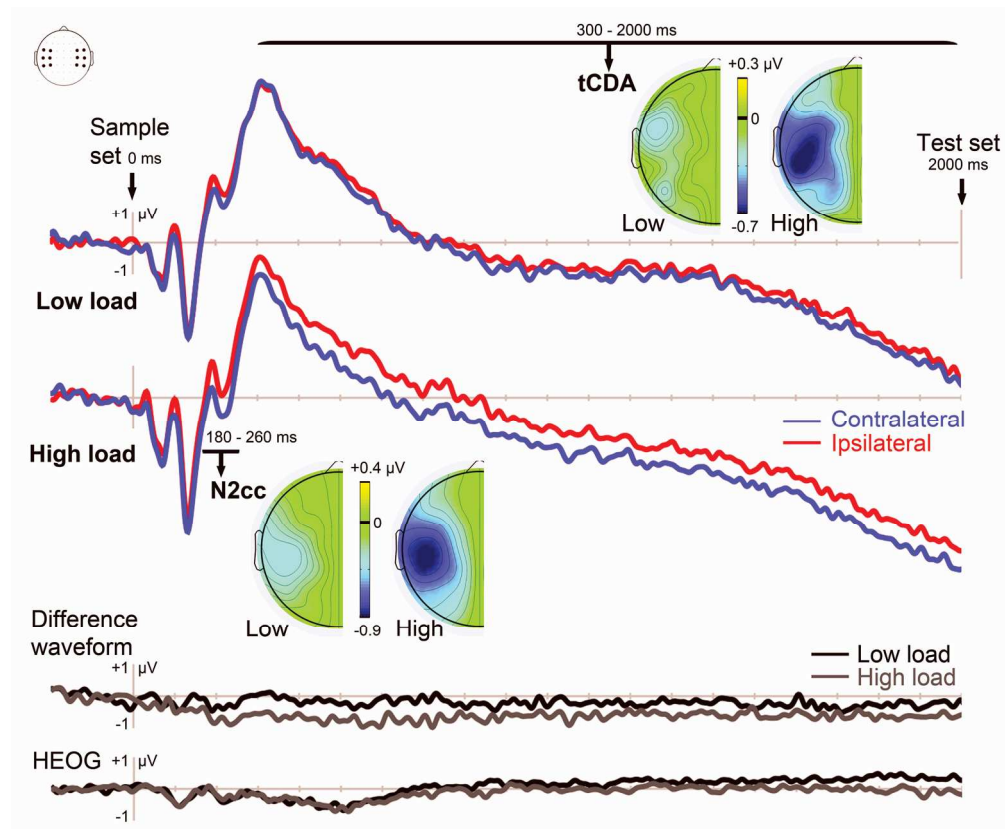


Figure 2. Grand mean ERPs elicited in the 2000 ms interval following sample stimulus onset in the low-load and high-load conditions. ERPs were averaged across lateral central electrode clusters contralateral (blue lines) and ipsilateral (red lines) to the hand where the memory task was performed. Difference maps show the topographical distribution of lateralized effects in the N2cc (bottom) and tCDA (top) time windows. These maps represent the amplitude difference of contralateral minus ipsilateral recordings, collapsed across blocks where the memory task was performed with the left or right hand. Enhanced contralateral negativities are shown in blue. The two bottom panels show difference waveforms for the low-load and high-load condition, obtained by subtracting electrodes ipsilateral to the task-relevant hand from contralateral electrodes, and HEOG difference waveforms, calculated by subtracting HEOG electrodes ipsilateral to the task-relevant hand from contralateral electrodes after artifact rejection. In these HEOG difference waves, any eye movements towards the task-relevant hand would be reflected by negative (downward) HEOG deflections.

180x148mm (300 x 300 DPI)

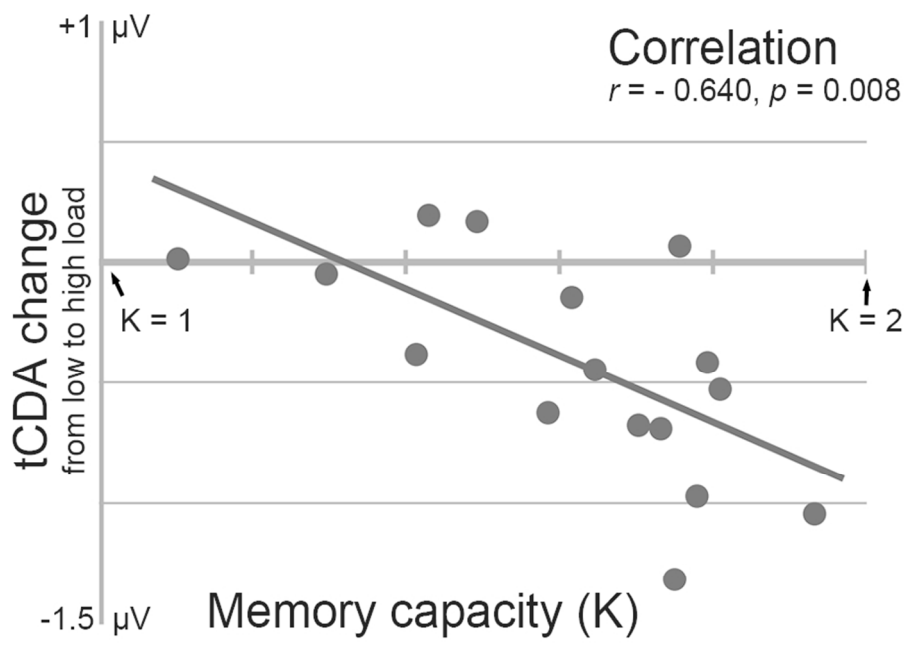


Figure 3. Correlation of individual participant’s tactile working memory capacity K (x-axis) and the increase of tCDA amplitudes in the high-load relative to the low-load condition measured for each participant (y-axis). K was calculated on the basis of individual performance in the high-load condition.  
86x61mm (300 x 300 DPI)

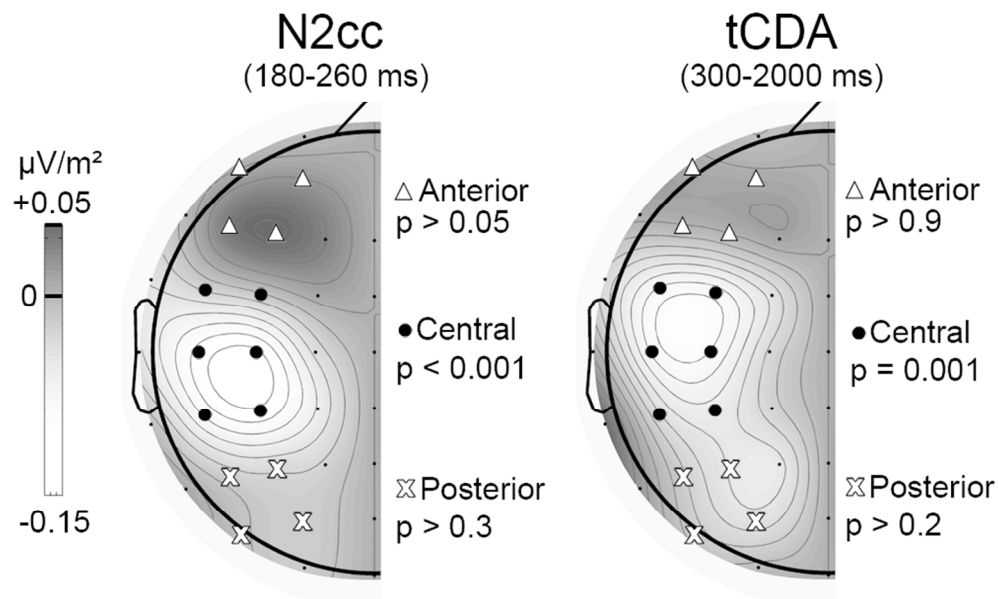


Figure 4. Grand mean current source density (CSD) topographical maps, showing the scalp distribution of lateralized effects in the N2cc and tCDA time windows. These maps represent the amplitude difference of contralateral minus ipsilateral recordings, collapsed across blocks where the memory task was performed with the left or right hand, and averaged across the low- and high-load conditions. Six electrodes at lateral central scalp regions (black dots) were averaged for each recording cluster (contra- and ipsilateral to the task-relevant hand). The presence of lateralized effects was also tested for different sets of electrodes over anterior (white triangles) and posterior (white crosses) scalp areas. Reliable lateralized effects were present only for the central electrode cluster.

86x52mm (300 x 300 DPI)